Chemistry
A European
Journal

Accepted Article

Title: A Doubly Dissipative System Driven by Chemical and Radiative Stimuli

Authors: Matteo Valentini, Federico Frateloreto, Matteo Conti, Roberta Cacciapaglia, Daniele Del Giudice, and Stefano Di Stefano

RESEARCH ARTICLE

A Doubly Dissipative System Driven by Chemical and Radiative Stimuli

Matteo Valentini,[a] Federico Frateloreto,[a] Matteo Conti,[a] Roberta Cacciapaglia,[a] Daniele Del Giudice[a] and Stefano Di Stefano*[a]

[a]   Matteo Valentini, Dr. Federico Frateloreto, Matteo Conti, Dr. Roberta Cacciapaglia, Dr Daniele Del Giudice and Prof. Stefano Di Stefano
        Department of Chemistry
        Università di Roma La Sapienza and ISB-CNR Sede Secondaria di Roma - Meccanismi di Reazione
        P.le A. Moro 5, I-00185 Roma, Italy
        E-mail: stefano.distefano@uniroma1.it

        Supporting information for this article is given via a link at the end of the document.

Abstract: The operation of a dissipative network composed of two or three different crown-ether receptors and an alkali metal cation can be temporally driven by the use (combined or not) of two orthogonal stimuli of different nature. More specifically, irradiation with light at a proper wavelength and/or addition of an activated carboxylic acid, are used to modulate the binding capability of the above crown-ethers towards the metal ion, allowing to control over time the occupancy of the metal cation in the crown-ether moiety of a given ligand. Thus, application of either or both of the stimuli to an initially equilibrated system, where the metal cation is distributed among the crown-ether receptors depending on the different affinities, causes a programmable change in the receptor occupancies. Consequently, the system is induced to evolve to one or more out-of-equilibrium states with different distributions of the metal cation among the different receptors. When the fuel is exhausted or/and the irradiation interrupted, the system reversibly and autonomously goes back to the initial equilibrium state. Such results may contribute to the achievement of new dissipative systems that, taking advantage of multiple and orthogonal stimuli, are featured with more sophisticated operating mechanisms and time programmability.

Introduction

The great effort that chemistry researchers are currently devoting to dissipative systems is mainly motivated by the ambition to achieve complex and abiotic molecular networks, whose properties can be controlled at will over the time.[1] A dissipative system (DS) consists of a unique molecule or of an ensemble of molecules, which is initially found in an equilibrium state (Figure 1A), and then is driven to an out-of-equilibrium state[2] by the consumption of a chemical species[3] (chemical stimulus, sometimes referred to as chemical fuel[4]) or the absorption of radiative energy (radiative stimulus). [5,6] The out-of-equilibrium state persists as long as the stimulus is present. After exhaustion of the latter (the chemical fuel is completely transformed into the waste product or the irradiation is interrupted), the system goes back to the initial equilibrium state. Varying the nature or the amount of the added chemical fuel or the irradiation time, one can have full control on the time spent by the system in the out-of-

equilibrium state, and this would be of paramount importance if such a state is associated with useful functional properties.

In most cases, the DSs appeared in the literature so far and including molecular switches[7] and motors,[8] self-assembly systems,[9] host-guest[10] and translocation systems, [11] dynamic libraries,[12] smart materials[13] and so on, take advantage of just one of the above two kinds of stimulus at a time, either chemical or radiative (Figure 1A).

As for DSs driven by the consumption of a chemical species, in recent years we showed that the operation of a series of systems based on the acid-base reaction can be easily driven by the use of activated carboxylic acids (ACAs), whose decarboxylation smoothly proceeds in the presence of a base promoter.[14] If the DS is endowed with one or more basic sites, upon addition of the ACA, it passes from a neutral resting state A to a protonated out-of-equilibrium state B (Figure 1B). Decarboxylation of the conjugate base of the ACA and consequent back proton transfer restore the initial state of the system, which turns to equilibrium. Remarkably, the duration of the out-of-equilibrium state can be modulated by varying the nature[15] and/or the amount of the added ACA.[16]

Here we report one of the rare cases[17] in which the operation of a dissipative system is driven by the contextual exploitation of both chemical and radiative stimuli. More specifically, in the present investigation we take advantage of two stimuli to achieve a multiple control of the dissipative system over the time. In other words, consumption of the fuel and absorption of the radiative energy interplay to bring the system into the desired out-of-equilibrium state (Figure 1C), which autonomously reverts to the equilibrium state when the stimuli aren't supplied anymore.

Results and Discussion

The system consists of a network based on different crown ethers, namely 4'-nitrobenzo-18-crown-6 (**1**),4'-aminobenzo-18-crown-6 (**2**), and azobis(benzo-15-crown-5) (**3**) shown in Figure 2. It is well-known that all of them have good affinities for
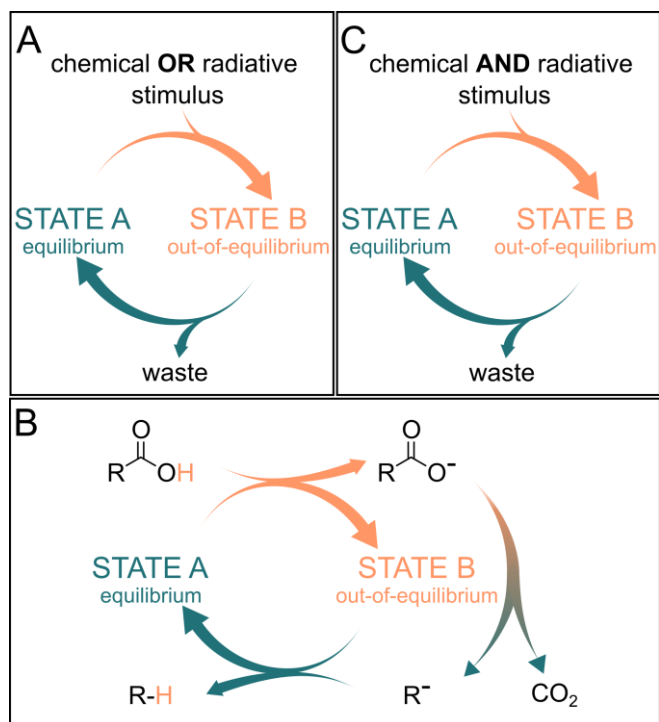
RESEARCH ARTICLE

Figure 1. A) A general dissipative system whose operation is driven by a chemical or a radiative stimulus. B) An acid-base operated dissipative system driven by the decarboxylation of an ACA. C) A dissipative system maintained in the desired out-of-equilibrium state by the contextual consumption of chemical species (for example an ACA) and absorption of light energy.

alkali and alkaline-earth cations due to multiple dipole-cation interactions, although some differences are expected.

For instance, we measured binding constants (K) of $1.6 \pm 0.1 \times 10^4$ M^{-1} and $1.6 \pm 0.6 \times 10^5$ M^{-1} for complexes **1**•Na$^+$ and **2**•Na$^+$ (perchlorate salt, NaClO$_4$), respectively, in methanol by means of UV-Vis spectroscopy (see SI, Figure S1 and S2). The lower affinity of **1** for Na$^+$ with respect to **2** is consistent with the electron-withdrawing properties of the nitro group, which differently from the electron-donating amino group present in **2**,
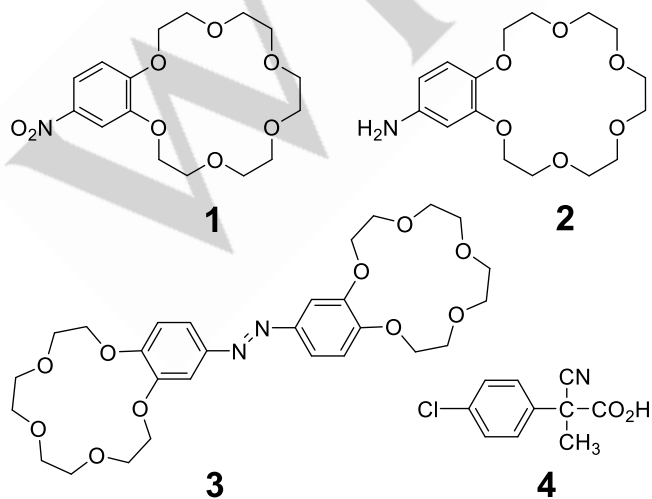

Figure 2. Structures of the compounds employed in the investigation.

subtracts charge density from the crown-ether moiety.

Thus, firstly, we designed a simple competition experiment (Figure 3A) in which **1**, **2** and NaClO$_4$ are added in methanol solution in equimolar amounts (5.0 mM). Under such conditions complexes **1**•Na$^+$ and **2**•Na$^+$, are formed in a 30:70 ratio. This ratio is calculated taking into account the variations of the chemical shift of the **1** ArOCH_2CH$_2$O- signal,[18] upon complexation of the Na$^+$ ion in the crown ether moiety,[19] and with the assumption derived from the above K values that, under these conditions, there is no unbound Na$^+$ in solution. This ratio is in a very good agreement with that calculated from the experimental values of the two association constants (see SI, Table S1). Addition of equimolar ACA **4** (5.0 mM) causes the immediate, partial protonation of the amino group of **2**. The just protonated -NH$_3^+$ ammonium group is now a strong electron-withdrawing group, and also due to electrostatic repulsion, the Na$^+$ cation is induced to shift from **2**H$^+$ to **1**, as clearly shown by ^{1}H-NMR spectra (Figure 3B, compare trace *a* with trace *b*). In the new out-of-equilibrium, transient state, the crown-ether occupancy ratio is overturned (**1**•Na$^+$ / **2**H$^+$•Na$^+$ ≈ 55:45). However, from now onward, decarboxylation and consequent back proton transfer take place, and at the end of the process the Na$^+$ is found back shifted to **2** in a reversible fashion (Figures 3B, traces *b-e*, and related black trace in Figure 3D). The process turns out to be fully reversible as demonstrated by the experiment shown in Figure 3C, where four subsequent cycles have been triggered by four successive additions of **4**. Remarkably, the higher the amount of added **4**, the higher the percentage of transiently translocated Na$^+$, the longer the time needed to return to the equilibrium, initial state (Figure 3D) since dissipation of **4** requires increasingly longer times.

The above dissipative process also works with other cations, such as potassium (trifluoromethanesulfonate salt, KOTf) and barium (perchlorate salt, Ba(ClO$_4$)$_2$), as reported in Figure 3E, although different translocation fractions and time durations are observed. With the exception of the runs carried out in the presence of excess acid, all the experimental data points were fitted with 1st order kinetic curves (k$_{obs}$ values are reported in the captions), which are in accordance with the expected first order decarboxylation mechanism.[7a,14,15a]

Secondly, we explored the possibility of a light-induced shift of the K$^+$ ion, between **1** and **3**. In this case, K$^+$ was preferred to Na$^+$ because of the too low affinity of the latter for receptor **3** in both its *trans* and *cis* forms, which would have hampered the experiment (*vide infra*).

Compound **3** was prepared following a literature procedure,[20] which exclusively leads to the *trans* isomer. It is well-known that irradiation of *trans*-**3** with light at the proper wavelength, allows the *trans* → *cis* isomerization of the N=N double bond. Taking into account the UV-Vis spectra of both *trans*-**3** and *cis*-**3** (see Figures S10 and S11, actually the spectrum in Figure S11 is related to a 93:7 *cis*/*trans* photo-stationary state), we decided to use a violet-lamp with emission centered at 390 nm for the *trans* → *cis* isomerization. Irradiation at such wavelength guarantees the highest efficiency of the *trans* → *cis* isomerization with the advantage that the radiation is not absorbed to any extent by the glass of the NMR tubes where the experiments are carried
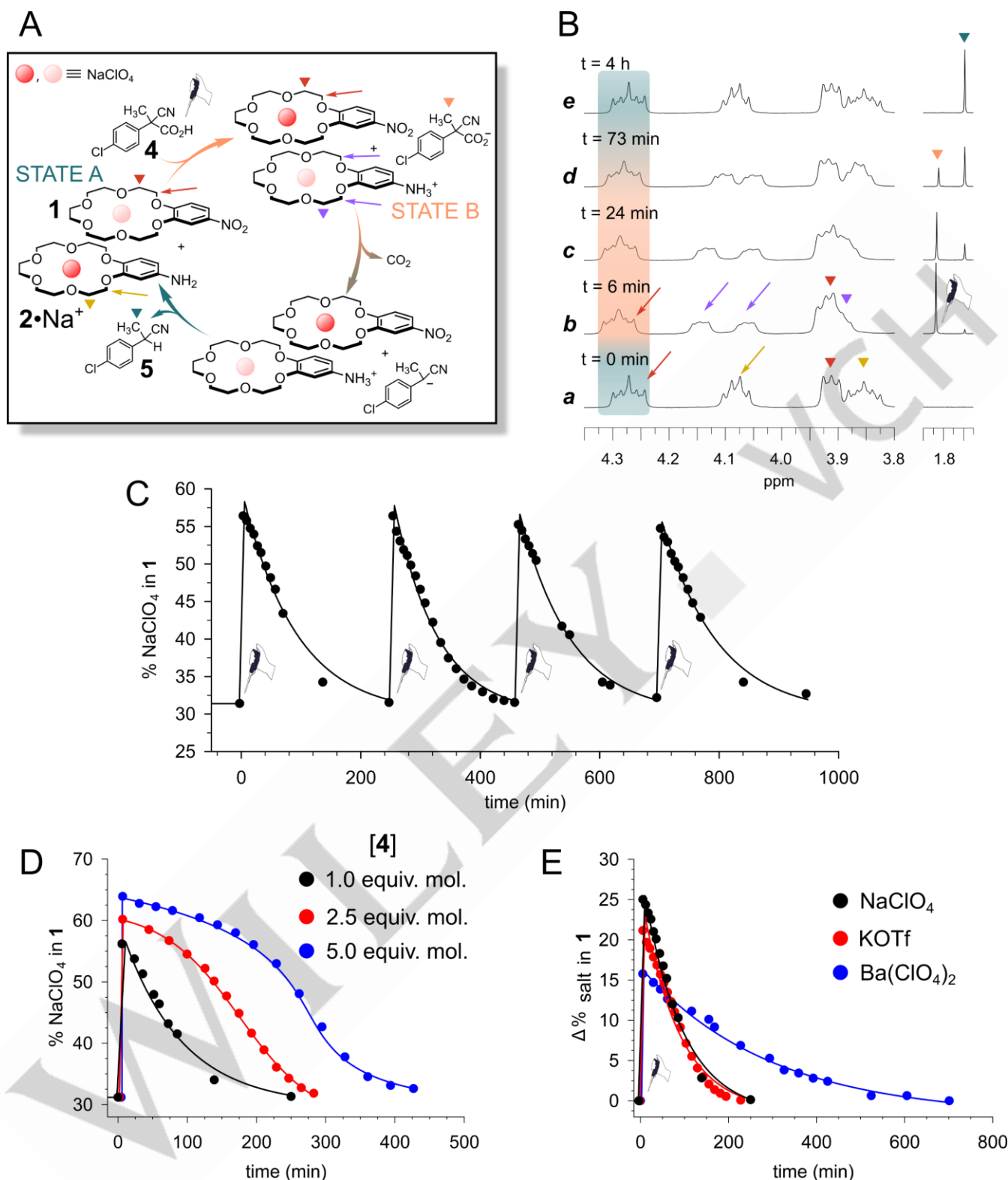
RESEARCH ARTICLE

Figure 3. A) Schematic cartoon showing the dissipative $2 \cdot Na^+ \rightarrow 1 \cdot Na^+ \rightarrow 2 \cdot Na^+$ occupancy change driven by **4** (the higher the intensity of the sphere color inside the crown-ether moiety, the larger its occupancy by the cation. H/D exchange in CD_3OD is omitted). B) The translocation is followed by monitoring the $ArOCH_2CH_2O$ ^1H NMR signals of **1** (red arrow), which are only influenced by Na^+ complexation (5.0 mM equimolar **1**, **2**, and $NaClO_4$; CD_3OD, 25 °C). C) Subsequent $2 \cdot Na^+ \rightarrow 1 \cdot Na^+ \rightarrow 2 \cdot Na^+$ occupancy change driven by successive shots of **4** (first shot, $k = 1.9 \pm 0.2 \ 10^{-4} \ s^{-1}$; second shot, $k = 2.3 \pm 0.2 \ 10^{-4} \ s^{-1}$; third shot, $k = 1.9 \pm 0.2 \ 10^{-4} \ s^{-1}$; fourth shot, $k = 1.8 \pm 0.2 \ 10^{-4} \ s^{-1}$). D) Effects of addition of increasing amount of **4** to drive the dissipative $2 \cdot Na^+ \rightarrow 1 \cdot Na^+ \rightarrow 2 \cdot Na^+$ occupancy change (black trace, $k = 1.9 \pm 0.2 \ 10^{-4} \ s^{-1}$, red and blue lines are guides to the eye). E) Different cations alternatively shifted between **2** and **1** (for the sake of clarity variation of **1** occupancy (Δ%) over the time is reported; black trace, $k = 1.9 \pm 0.2 \ 10^{-4} \ s^{-1}$; red trace, $k = 2.0 \pm 0.2 \ 10^{-4} \ s^{-1}$; blue trace, $k = 5.7 \pm 0.6 \ 10^{-5} \ s^{-1}$). See Figures S4-9 for more details.
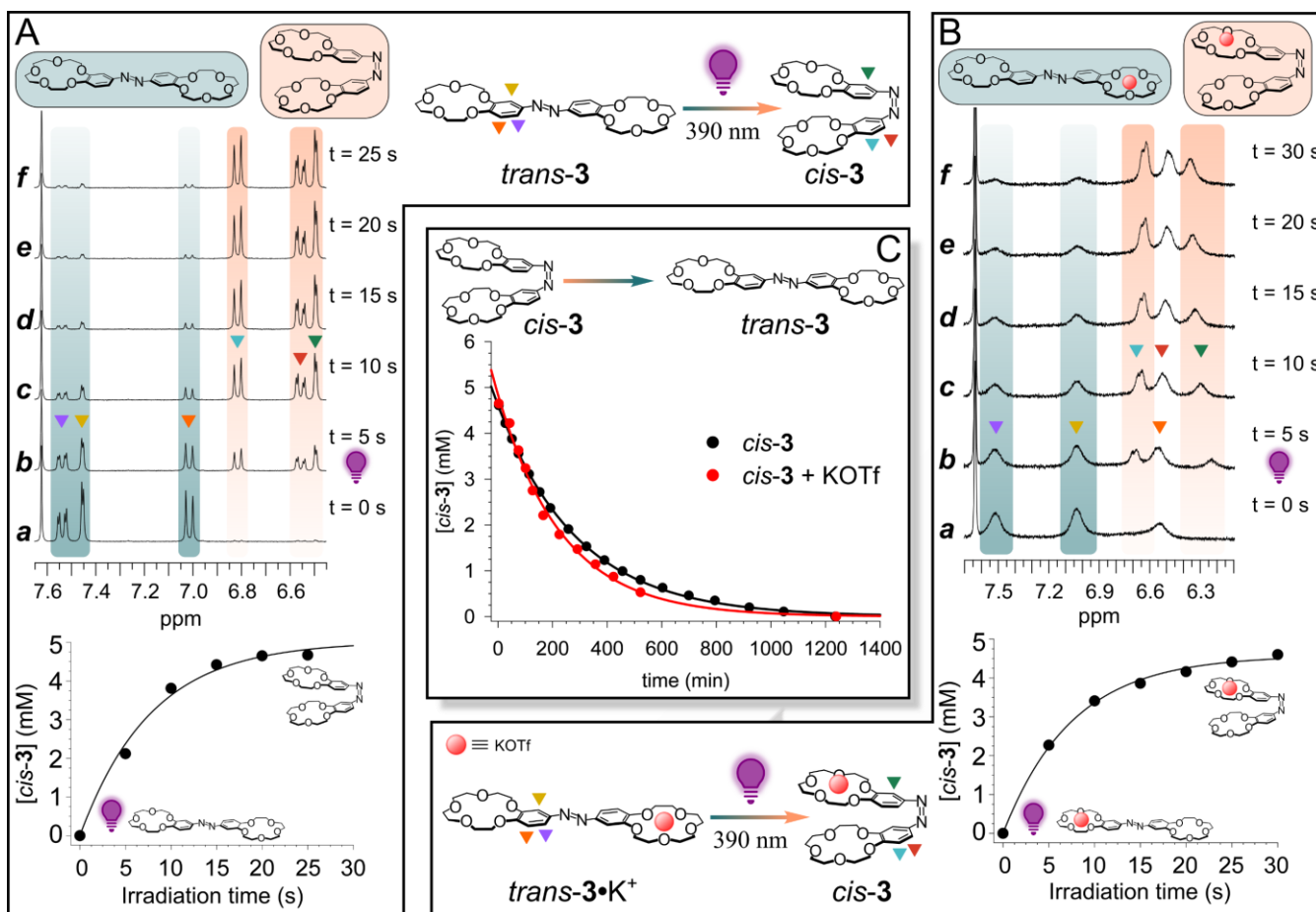
Figure 4. Kinetically first-order *trans* → *cis* isomerization of 5.0 mM *trans*-**3** (CD$_3$OD / CDCl$_3$ 60:40, T = 25 °C, violet-lamp irradiation) in the absence ($k = 1.3 \cdot \pm 0.1$ 10^{-1} s^{-1}) (A) and in the presence ($k = 1.1 \cdot \pm 0.1$ 10^{-1} s^{-1}) (B) of 5.0 mM KOTf. In the former case the process takes 25 s, in the latter one 30 s. In both cases the photo-stationary state is a *cis/trans* 93:7 mixture. Both in the absence and presence of equimolar KOTf, the kinetically first-order thermal reversion requires more than 20 h (black trace, $k = 5.7 \cdot \pm 0.6$ 10^{-5} s^{-1}; red trace, $k = 7.0 \cdot \pm 0.7$ 10^{-5} s^{-1}) (C). See Figures S12-15 for more details.

out. Figure 4A and 4B show selected ^{1}H NMR spectra and the kinetic profile for the related *trans*-**3** → *cis*-**3** conversion, in the absence or presence of KOTf, respectively. The use of the CD$_3$OD / CDCl$_3$ 60:40 (v/v) mixture was dictated by the low solubility of *trans*-**3** in pure methanol. It is apparent that, under the adopted conditions, 25 and 30 seconds are enough to reach the photo-stationary state in the absence or presence of K$^+$, respectively. The composition of the photo-stationary states is 93:7 *cis/trans* in both cases. Thermal reversion to the *trans* form takes more than 20 h in both cases (Figure 4C).

When **1**, *trans*-**3**, and KOTf were added in CD$_3$OD / CDCl$_3$ 60:40 in equimolar amounts (5.0 mM), the potassium cation was unexpectedly mainly found complexed in *trans*-**3** (nearly 76% in *trans*-**3** and 24% in **1**, Figure 6A, state **A**). This finding is in fact consistent with the rough estimation of K value 10^5 M^{-1} for **1**•K$^+$ and quantitative association between *trans*-**3** and K$^+$ in CD$_3$OD / CDCl$_3$ 60:40 (see SI, Table S1). We tentatively ascribe such a result to the formation of 2:2 (**I**) or polymeric (**II**) sandwich adducts of the kind depicted in Figure 5, with preference to the arrangement **II** in consideration of the NMR signal broadening when *trans*-**3** is saturated with KOTf (see SI, Figure S21).

In the co-presence of **1**, a longer irradiation time is needed to reach the *cis* / *trans* **3** photo-stationary state, which is obtained only after 60 seconds (see black trace in Figure 6C). Moreover, this photo-stationary state has a different composition, estimated as *cis*-**3** /*trans*-**3** 56:44. However, the 60 s irradiation of the above 5.0 mM equimolar solution of **1**, *trans*-**3** and KOTf causes the *trans*-**3** → *cis*-**3** isomerization with a consequent change of the K$^+$ occupancy of the crown ether moieties (Figure 6A, state **B**). The *cis* form of **3** was in fact found to be a poor binder for the potassium, probably due to a reduced availability of the intermolecular sandwich arrangement.
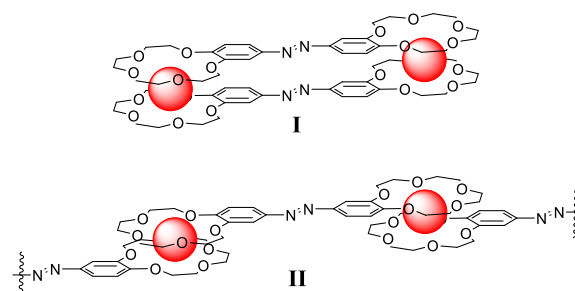

Figure 5. Different sandwich-binding modes of K$^+$ by **3**.

4

RESEARCH ARTICLE

Thus, in trace *b* of Figure 6B, recorded after 3 minutes from irradiation, the potassium cation has been transferred to **1** (**1** occupancy has passed from 24% to 51%). However, as thermal relaxation of *cis*-**3** to *trans*-**3** takes place, the cation reversibly translocates back to *trans*-**3** and the process is complete after 23 h (trace *e* of Figure 6B). Eventually, Figure 6C and 6D show the kinetic profile of the whole light-induced translocation process. Specifically, the initial and fast, light-promoted A→B translocation is shown by the red trace in Figure 6C and the slower, thermal back B→A translocation by the red trace in Figure 6D.

Thus, differently from what occurs in the previous experiment, in this case a light stimulus instead of a chemical one has been used to drive the reversible motion of the K$^+$ cation.

Then, we designed a more structured experiment in which both chemical and radiative stimuli drive the operation of the translocation system (see Figure 7A). **1**, **2**, *trans*-**3**, and KOTf are added in equimolar amounts (5.0 mM) in a CD$_3$OD / CDCl$_3$ 60:40 solution.[21] Under such conditions, the K$^+$ occupancy of receptor **1** is as low as 10% (see Figure 7B trace *a* and Figure 7C at t = 0), since **1** is the poorest binder in the lot. From the binding data collected (*vide supra* and Table S1), the potassium cation should be mainly hosted by *trans*-**3** (Figure 7A, state A). Then, the solution is irradiated for a total time of 60 sec at 390 nm and K$^+$ is induced to pass from **3**, now in the *cis* form,[22] to **1** and **2** (Figure 7A, state B), with a preference for the latter due to the higher affinity of K$^+$ for **2** than for **1** (*vide supra* and Table S1). Nonetheless in the new state B, the K$^+$ occupancy of **1** is 30% as shown by trace *b* of Figure 7B and by the inset of Figure 7C. Note that such state B is not an equilibrium state. In fact the thermal reversion *cis*-**3** → *trans*-**3** would spontaneously bring back the system to the initial state A after 23 h (see Figure 6D). But at this point, the addition of ACA **4** after 3 min from the end of irradiation causes an additional fraction of the K$^+$ cation to rapidly move from **2**H$^+$ to **1**, bringing the system into the further out-of-equilibrium state B' (Figure 7A), where 46% **1** is occupied by the K$^+$ cation (trace *c* of Figure 7B and Figure 7C at t = 7 min). From now onward, decarboxylation and thermal reversion take place (Figure 7B, traces *d* to *f*), and, at the end of the two processes the translocation system is in its initial equilibrium state A, with **1** occupancy at 10 % again (compare traces *a* and *f* of Figure 7B, which are superimposable, apart from the signals due to the waste 2-cyano-2-(4'-chlorophenyl)ethane (**5**)).

Since decarboxylation of **4** is faster than thermal *cis*-**3** → *trans*-**3** reversion (t$_{1/2}$ = 79 min and 3 h, respectively), it is expected that going from state B' to state A of Figure 7A, there will be an intermediate out-of-equilibrium state in which K$^+$ again prefers ligand **2** among the other ones, as happens in state B.

Eventually, another doubly dissipative experiment was carried out inverting the order of the stimuli supply. To a 5.0 mM equimolar solution of **1**, **2**, *trans*-**3**, and KOTf in CD$_3$OD / CDCl$_3$ 60:40, firstly 5.0 mM ACA **4** was added, and then, after 5 minutes from addition, the solution was irradiated for 60 s at 390 nm. As shown in Figure 8, the state B' reached just after the supply of both stimuli is perfectly superimposable to the state B' of Figure 7C in terms of K$^+$ occupancy of **1**. The same holds for the relaxing process to state A.
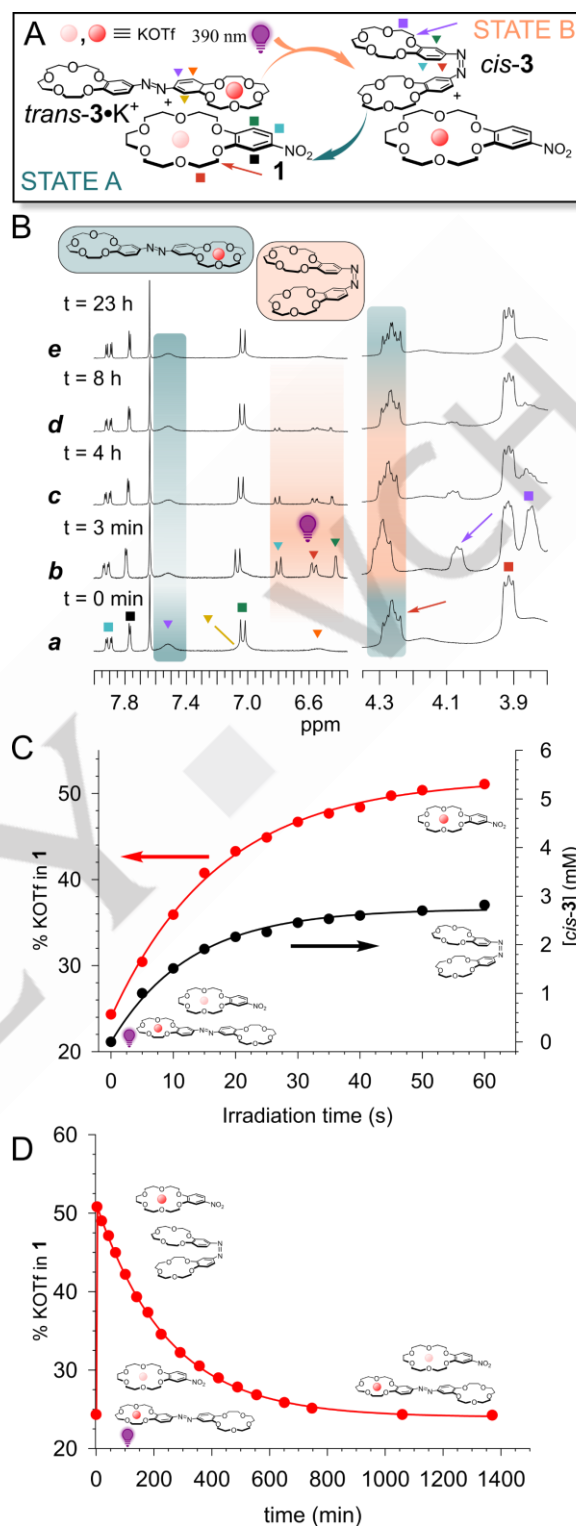

Figure 6. A) Light-induced shift of K$^+$ from **3** to **1** and back again to **3** (the higher the intensity of the sphere color inside the crown-ether moiety, the larger its occupancy by the cation). B) Trace *a*: system in state A (see panel A); trace *b*: system after 60 s irradiation at 390 nm, state B (see panel A); traces *c-e*: subsequent relaxation to state A. C) *Trans* to *cis* isomerization of 5.0 mM *trans*-**3** in the presence of equimolar **1** and KOTf (black trace, $k = 7.9 \cdot \pm 0.8 \, 10^{-2} \, s^{-1}$) and consequent K$^+$ translocation to **1** (red trace, $k = 5.7 \cdot \pm 0.6 \, 10^{-2} \, s^{-1}$). D) Back-translocation of K$^+$ from **1** to *trans*-**3** as monitored by K$^+$ occupancy variation in **1** ($k = 6.8 \cdot \pm 0.7 \, 10^{-5} \, s^{-1}$). See Figures S16-17 for more details.
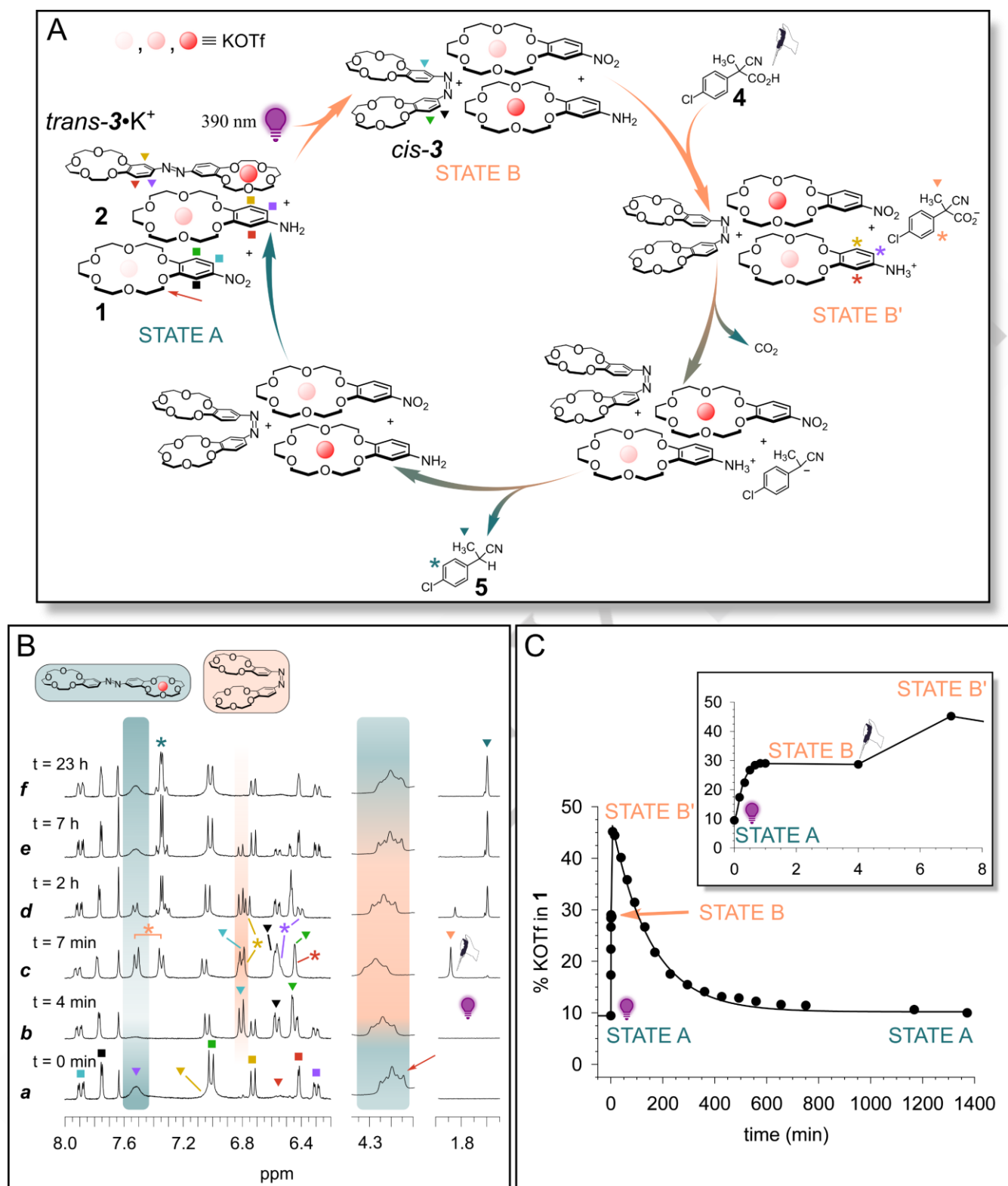
5

Figure 7. A) Schematic representation of the doubly dissipative occupancy change of the K$^+$ cation driven by light and fuel **4** (the higher the intensity of the sphere color inside the crown-ether moiety, the larger its occupancy by the cation. H/D exchange in CD$_3$OD-CDCl$_3$ 60:40 is omitted). B) ^{1}H NMR monitoring of the doubly dissipative process. Trace *a*: equimolar solution of **1**, **2**, *trans*-**3** and KOTf 5.0 mM each in CD$_3$OD/CDCl$_3$ 60:40 (t = 0); trace *b*: solution of trace *a* after irradiation at 390 nm (t = 4 min); trace *c*: solution of trace *b* after addition of 5.0 mM ACA **4** (t = 7.7 min); traces *d-f* back translocation to initial, resting state. C) K$^+$ occupancy of **1** during the process as a function of time (for decay $k = 1.1 \pm 0.1 \ 10^{-4} \ s^{-1}$). The inset is the zoom of the region from 0 to 8 min (in particular time from 0 to 1 min is related to irradiation time at 390 mm, $k = 4.9 \pm 0.5 \ 10^{-2} \ s^{-1}$). See Figures S18-19 for more details.
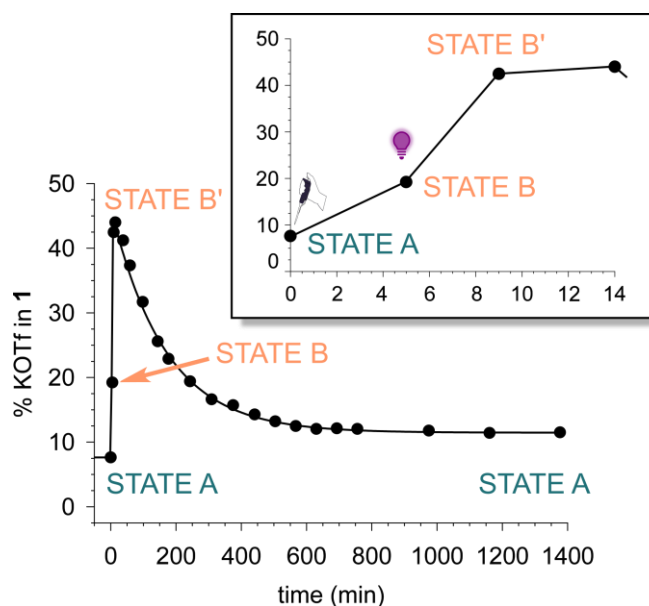
RESEARCH ARTICLE

Figure 8. K+ occupancy of **1** as a function of time (for decay $k = 1.0 \pm 0.1 \ 10^{-4}$ s^{-1}). The initial ACA **4** supply at t = 0, is followed by the 60 sec irradiation at t = 5 min (see Figure S20 for related ^{1}H NMR spectra; initial conditions are **1**, **2**, *trans*-**3**, and KOTf 5.0 mM each in CD$_3$OD / CDCl$_3$ 60:40). The inset is the zoom of the region from 0 to 14 min.

Conclusion

In this report we have shown that two different stimuli, a chemical stimulus (fuel **4**) and a light stimulus, can be used to drive the operation of a complex translocation network. More specifically, it was possible to control over the time the K+ cation movements among the crown-ether moieties of different crown-ether based receptors. Irradiation with light at the proper wavelength (λ_{max} = 390 nm) and supply of ACA **4** fuel, allow to control the fraction of the different crown-ether moieties occupied by the alkali metal cation in a dissipative fashion. After interruption of the irradiation and exhaustion of the chemical fuel, the system autonomously reverts to the initial equilibrium state. The composition and duration of the out-of-equilibrium states can be varied in terms of irradiation times and amount of added fuel. Remarkably, as shown in Figure **7** (and **8**), subsequent supplies of light and fuel **4** (and *vice-versa*) allow to alternatively control at will the occupancy of the K+ among the crown-ethers in the lot. Thus, for the first time two independent and orthogonal stimuli[23] contextually drive a dissipative system by acting on two independent reversible processes (namely, the -NH$_2$ → -NH$_3$$^+$ → -NH$_2$ and *trans*-**3** → *cis*-**3** →*trans*-**3** transformations).

Hopefully these findings will contribute to develop increasingly complex dissipative systems, whose functional properties can be controlled over time following the will of the experimenter.

Experimental section

Instrument and Methods. ^{1}H NMR spectra were recorded on a 300 MHz spectrometer. The spectra were internally referenced to the residual proton signal of the solvent at 3.31 ppm for CD$_3$OD or at 7.26 ppm for CDCl$_3$. All the experiments were carried out in NMR tubes at constant temperature.UV-Vis measurements were carried out in the thermostated (25 °C) cell compartment of a double-beam spectrophotometer. A Kessil PR160L-390 nm lamp (λ_{em}=390 nm) was used to promote the *trans* to *cis* photoisomerization of **3**. An NMR tube-sealing manifold was used to carry out freeze-pump-thaw cycles. The experiments were performed under an argon atmosphere.

Materials. All reagents and solvents were purchased at the highest commercial quality and were used without further purification, unless otherwise stated. All NMR solvents were stored in a desiccator loaded with activated silica gel Rubin. CDCl$_3$ was filtered on activated basic alumina gel in order to remove acidic impurities, and then dried over molecular sieves (3 Å) for 24 h. Molecular sieves were activated at 300 °C for 24 h prior to use. 2-cyano-2-(4'-chloro)phenylpropanoic acid (**4**) was available from a previous investigation.[15a] **2** was synthesized following a literature procedure[20]. *Trans*-**3** was synthesized adapting a literature procedure[24], and characterization is in accordance with that reported in the literature[25] (see SI for details).

Supporting Information

The authors have cited additional references within the Supporting Information.[24, 25]

Conflict of interest

The authors declare no conflict of interest.

References

[1] N. Giuseppone, A. Walther, *Out-of-Equilibrium (Supra)molecular Systems and Materials*, Wiley-VCH, **2021**.

[2] As pointed out by Hartley and co-workers (see ref 3b), the term "out-of-equilibrium" can simply refer to a "system which is not at equilibrium, in the sense that it is under kinetic control and changing with time".

[3]   a) C. Biagini, S. Di Stefano, *Angew. Chem. Int. Ed* **2020**, *59*, 8344-8354; b) L. S. Kariyawasam, M. M. Hossain, C. S. Hartley, *Angew. Chem. Int. Ed.* **2021**, *60*, 12648-12658; c) S. Borsley, D. A. Leigh, B. M. W. Roberts, *Nat. Chem.* **2022**, *14*, 728-738.

[4]   The term "fuel" is frequently debated in the recent literature of the field. Throughout this paper, with fuel we will indicate a chemical stimulus capable of maintaining a dissipative system based on a well-behaved chemical reaction cycle in an out-of-equilibrium state (see ref 14).

[5]   a) J. Volarić, W. Szymanski, N. A. Simeth, B. L. Feringa, *Chem. Soc. Rev* **2021**, *50*, 12377-12449; b) R. Costil, M. Holzheimer, S. Crespi, N. A. Simeth, B. L. Feringa, *Chem. Rev.* **2021**, *121*, 13213-13237. c) S. Corra, M. Tranfić Bakić, J. Groppi, M. Baroncini, S. Silvi, E. Penocchio, M. Esposito, A. Credi, *Nat. Nanotechnol.* **2022**, *17*, 746-751.

[6]   M. Weißenfels, J. Gemen, R. Klajn, *Chem* **2021**, *7*, 23-37.

[7]   a) J. A. Berrocal, C. Biagini, L. Mandolini, S. Di Stefano, *Angew. Chem. Int. Ed.* **2016**, *55*, 6997 – 7001; *Angew. Chem.* **2016**, *128*, 7111 – 7115. b) I. M. Jayalath, M. M. Gerken, G. Mantel, C. S. Hartley, *J. Org. Chem.* **2021**, *86*, 12024–12033; c) S. Borsley, D. A. Leigh, B. M. W. Roberts, *J. Am. Chem. Soc.* **2021**, *143*, 4414–4420. d) E. Spatola, F. Rispoli, D. Del Giudice, R. Cacciapaglia, A. Casnati, L. Marchiò, L. Baldini, S. Di Stefano, *Org. Biomol. Chem.* **2021**, *20*, 132–138. e) D. Del Giudice, M. Valentini, C. Sappino, E. Spatola, A. Murru, G. Ercolani, S. Di Stefano, *J. Org. Chem.* **2023**, *88*, 4379-4386.

[8]   a) M. R. Wilson, J. Solà, A. Carlone, S. M. Goldup, N. Lebrasseur, D. A. Leigh, *Nature* **2016**, *534*, 235-240; b) S. Erbas-Cakmak, S. D. P. Fielden, U. Karaca, D. A. Leigh, C. T. McTernan, D. J. Tetlow, M. R. Wilson, *Science* **2017**, *358*, 340-343; c) S. Borsley, E. Kreidt, D. A. Leigh, B. M. W. Roberts, *Nature* **2022**, *604*, 80-85. d) K. Mo, Y. Zhang, Z. Dong, Y. Yang, X. Ma, B. L. Feringa, D. Zhao, *Nature* **2022**, *609*, 293-298.

[9]   a) K. Das, L. Gabrielli, L. J. Prins, *Angew. Chem. Int. Ed.* **2021**, *60*, 20120-202143; b) A. Sharko, D. Livitz, S. De Piccoli, K. J. M. Bishop, T. M. Hermans, *Chem. Rev.* **2022**, *122*, 11759–11777; c) C. Sharma, I. Maity, A. Walther, *Chem. Commun.* **2023**, *59*, 1125-1144.

[10]   a) D. Del Giudice, E. Spatola, M. Valentini, C. Bombelli, G. Ercolani, S. Di Stefano, *Chem. Sci.*, **2021**, *12*, 7460-7466; b) F. Rispoli, E. Spatola, D. Del Giudice, R. Cacciapaglia, A. Casnati, L. Baldini, S. Di Stefano, *J. Org. Chem.* **2022**, *87*, 3623-3629; c) M. P. van der Helm, G. Li, M. Hartono, R. Eelkema, *J. Am. Chem. Soc.* **2022**, *144*, 9465-9471.

[11]   a) A. Ghosh, I. Paul, M. Schmittel, *J. Am. Chem. Soc.* **2019**, *141*, 18954-18957; b) F. Frateloreto, F. Tavani, M. Di Berto Mancini, D. Del Giudice, G. Capocasa, I. Kieffer, O. Lanzalunga, S. Di Stefano, P. D'Angelo, *J. Phys. Chem. Lett.* **2022**, *13*, 5522-5529; c) A. Ghosh, I. Paul, M. Schmittel, *J. Am. Chem. Soc.* **2021**, *143*, 5319-5323; d) M. M. Wootten, S. Tshepelevitsh, I. Leito, J. A. Clayden, *Chem. Eur. J.* **2022**, e202202247.

[12]   a) M. M. Hossain, J. L. Atkinson, C. S. Hartley *Angew. Chem. Int. Ed.* **2020**, *59*, 13807–13813; b) S. Yang, G. Schaeffer, E. Mattia, O. Markovitch, K. Liu, A. S. Hussain, J. Ottelé, A. Sood, S. Otto, *Angew. Chem. Int. Ed.* **2021**, *60*, 11344-11349; c) M. G. Howlett, R. J. H. Scanes, S. P. Fletcher, *JACS Au* **2021**, *1*, 1355-1361; d) C. M. E. Kriebisch, A. M. Bergmann, J. Boekhoven, *J. Am. Chem. Soc.* **2021**, *143*, 7719-7725; e) D. Del Giudice, M. Valentini, G. Melchiorre, E. Spatola, S. Di Stefano, *Chem. Eur. J.* **2022**, *28*, e202200685; f) D. Del Giudice, E. Spatola, M. Valentini, G. Ercolani, S. Di Stefano, *ChemSystemsChem* **2022**, *4*, e202200023.

[13]   a) B. Zhang, I. M. Jayalath, J. Ke, J. L. Sparks, C. S. Hartley, D. Konkolewicz, *Chem. Commun.* **2019**, *55*, 2086-2089; b) N. Singh, A. Lopez-Acosta, G. J. M. Formon, T. M. Hermans, *J. Am. Chem. Soc.* **2021**, *144*, 410-415; c) N. Singh, B. Lainer, G. J. M. Formon, S. De Piccoli, T. M. Hermans, *J. Am. Chem. Soc.* **2020**, *142*, 4083-4087; d) G. Fusi, D. Del Giudice, O. Skarsetz, S. Di Stefano, A. Walther, *Adv. Mater.* **2023**, *35*, 2209870; e) X. Chen, M. A. Würbser, J. Boekhoven, *Acc. Mater. Res.* **2023**, DOI: 10.1021/accountsmr.2c00244.

[14]   D. Del Giudice, S. Di Stefano, *Acc. Chem. Res.* **2023**, *56*, 889-899.

[15]   a) C. Biagini, S. Albano, R. Caruso, L. Mandolini, J. A. Berrocal, S. Di Stefano, *Chem. Sci.* **2018**, *9*, 181–188; b) P. Franchi, C. Poderi, E. Mezzina, C. Biagini, S. Di Stefano, M. Lucarini, *J. Org. Chem.* **2019**, *84*, 9364−9368.

[16]   a) C. Biagini, F. Di Pietri, L. Mandolini, O. Lanzalunga, S. Di Stefano, *Chem. Eur. J.* **2018**, *24*, 10122–10127; b) C. Biagini, G. Capocasa, V. Cataldi, D. Del Giudice, L. Mandolini, S. Di Stefano, *Chem. Eur. J.* **2019**, *25*, 15205–15211; c) C. Biagini, G. Capocasa, D. Del Giudice, V. Cataldi, L. Mandolini and S. Di Stefano, *Org. Biomol. Chem.* **2020**, *18*, 3867–3873.

[17]   Previous examples in which both consumption of chemical species and absorption of light radiation are used to drive the operation of dissipative systems are: a) J. Deng, D. Bezold, H. J. Jessen, A. Walther, *Angew. Chem. Int. Ed.* **2020**, *59*, 12084-12092, but in this case one stimulus consists of a light irradiation that induces an irreversible variation; b) F. Nicoli, M. Curcio, M. T. Bakić, E. Paltrinieri, S. Silvi, M. Baroncini, A. Credi, *J. Am. Chem. Soc.* **2022**, *144*, 10180−10185, where an autonomous rotaxane-based switch is operated by a light and a base stimulus, but only the former is dissipative in nature; c) C. Chen, Z. Guan, *Chem. Eur. J.* **2023**, e202300347, but in this case both the stimuli must be used in order to have reversibility; d) S. Chowdhuri, S. Das, R. Kushwaha, T. Das, B. K. Das, D. Das, *Chem. Eur. J.* **2023**, e202203820, but in this case the two stimuli are alternatively used to induce the same reversible variation.

[18]   Na+ (or K+ or Ba^{2+}) occupancy in **1** is calculated as the ratio $(\delta_{obs} - \delta_{free}) / (\delta_{sat} - \delta_{free}) \times 100$, where δ_{obs} is the observed chemical shift of the **1** ArOC*H*$_2$CH$_2$O- signal (in ppm) in the presence of NaClO$_4$ (or KOTf or Ba(ClO$_4$)$_2$), δ_{free} is that in the absence of the salt, and δ_{sat} is the chemical shift of the same signal when receptor **1** is saturated by NaClO$_4$ (or KOTf or Ba(ClO$_4$)$_2$).

[19]   A blank experiment in which 5.0 mM acid **4** was added to 5.0 mM **1** in CD$_3$OD, showed no trace of **4** decarboxylation and, more importantly, no shift of any of the ^{1}H NMR signals belonging to receptor **1**, upon the addition of the acid (see SI, Figure S3).

[20]   R. Cacciapaglia, S. Di Stefano, L. Mandolini, *J. Am. Chem. Soc.* **2003**, *125*, 2224 – 2227.

[21]   In this case the solution was subjected to freeze-pump-thaw vacuum-argon cycles since the presence of oxygen was found to be detrimental to the system operation. This was not necessary in all other cases.

[22]   Interestingly, in the co-presence of **1**, **2** and KOTf (5.0 mM each), although the time needed to reach the photo-stationary state remains as long as 60 s, the *cis* / *trans* **3** composition of the photo-stationary state comes back to be as high as 91:9.

[23]   As a matter of fact, protonation of **2** to **2**H+ causes a change of its absorption spectrum with a consequent variation of the amount of radiation available to **3** when the solution is irradiated at 390 nm. This means that, at least in principle, the two stimuli may be not perfectly orthogonal.

[24]   N. A. Noureldin, J. W. Bellegarde, *Synthesis* **1999**, *6*, 939 – 942.

[25]   S. Shinkai, T. Nakaji, T. Ogawa, K. Shigematsu, O. Manabe, *J. Am. Chem. Soc.* **1981**, *103*, 111-115.

WILEY-VCH

RESEARCH ARTICLE

Entry for the Table of Contents
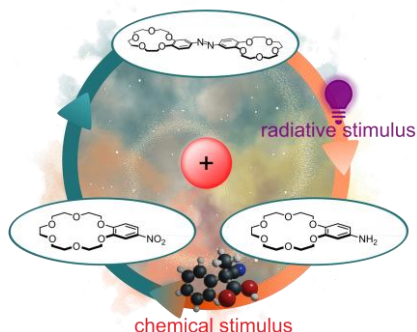
The motions of an alkali cation from and to the crown-ether moieties of different ligands (up to three) is controlled over time and in a dissipative fashion by contextually employing two orthogonal stimuli, namely a radiative one and a chemical one. When the stimuli are no longer supplied, moving from out-of-equilibrium states, the system reversibly returns to its equilibrium state.

Institute and/or researcher Twitter usernames: @S__DI_STEFANO; @SupRaLabRome; @ValMatteo_; @FedeFrateloreto; @Daniele_DelG